A new TDR waveform analysis approach for soil moisture profiling using a single probe

D. Moret*, J.L. Arrúe, M.V. López, R. Gracia

Departamento de Edafología, Estación Experimental de Aula Dei, Consejo Superior de Investigaciones Científicas (CSIC), PO Box 202, 50080 Zaragoza, Spain

* Corresponding author. Tel.: +34-976-716095; fax: +34-976-716145

E-mail address: david@eead.csic.es

ABSTRACT

Time Domain Reflectometry (TDR) has been widely accepted as a reliable technology for the measurement of volumetric water content (θ) in soils. Here we present a new procedure for the graphical interpretation of TDR waveforms to determine the variation of the apparent dielectric constant (K) along a single TDR probe in non-conducting media and its application for profiling the moisture content in soils. The method is based on the influence of K on the reflection coefficient (ρ) and travel time (t) of the TDR signal along a transmission line. A $\rho(t)$ function is initially defined for a length l of 10 cm and plotted together with the TDR waveform for a three-rod probe of length L (L= nl). The interception point of both lines defines t_{1l} as the reference time to build a second $\rho(t)$ line that intercepts the waveform at time t_{2l}. By repeating this process iteratively, a series of $\rho(t)$ lines intercepting the TDR trace at times t_{3l}, t_{4l},......and t_{nl} is obtained, making it possible to calculate K for apparent probe lengths equal to l, $2l$, $3l$.....and nl. To test the consistency of the method, two sand column experiments were conducted with two different TDR probe geometries. A total of 144 values of K were measured during a wetting and draining cycle of the sand column with vertical 10-, 20-, 30-, and 40-cm long three-wire uncoated TDR probes (diameter d: 2.8 mm; spacing of the outer conductors s: 32 mm) and 10-, 20-, 40-, and 60-cm long coated TDR probes (d: 10 mm; s: 80 mm) using the standard double reflection waveform analysis. A satisfactory relationship (R^2 = 0.99) was found between these K values and those obtained for the same depths by the proposed method applied to the 40- and 60-cm long probe, respectively. In this case, a probe-specific correction factor was used for the different probe geometries. Likewise, an excellent match was found between the θ profiles measured in the sand column applying the new approach to the 60-cm long probe and the θ profiles measured with horizontal probes placed at 10, 20, 30 and 50 cm depth. The results show that the proposed method is sound and suitable for determining the variation of K at fixed intervals along a single probe and therefore for soil water content profiling.

Keywords: Time domain reflectometry; Dielectric constant; Reflection coefficient; Characteristic probe impedance; Soil water content.

1. INTRODUCTION

Knowledge of soil water content and its distribution in the unsaturated zone is of paramount importance in many soil-related studies involving disciplines such as soil science, agriculture, forestry and hydrology. Time domain reflectometry (TDR) has become a worldwide standard method for the accurate, quick and non-destructive measurement of volumetric soil water content (θ) (Ferré and Topp, 2002).

Basically, a TDR instrument launches a fast-rise electromagnetic pulse (EM) along a coaxial cable, which carries the pulse to a probe embedded in the soil or porous medium of measurement. The pulse is displayed as a TDR waveform in which the voltage (V) or reflection coefficient (ρ) is a function of time (t). The travel time of the TDR pulse along the probe depends on the apparent dielectric constant of the soil (K) in the vicinity of the probe, which in turn is highly correlated with θ (Topp et al., 1980; Roth et al., 1990; Yu et al., 1997). In general, the measurement of t relies on the graphical interpretation of the waveform reflected from the probe length, i.e. the double-tangent waveform analysis procedure (Herkelrath et al., 1991).

As reviewed by Ferré and Topp (2002), the measurement of soil water content profiles by TDR can be made using i) vertical TDR probes of different lengths, ii) horizontally embedded probes, and iii) a vertical single TDR probe. All of these techniques present several advantages and limitations. The use of vertically installed multiple-length probes thus involves different locations, which increases the error associated with soil spatial variability. The installation of horizontal probes at different depths is less affected by lateral spatial variations but entails opening a trench in the soil and is consequently prone to significant errors in the presence of vertical heterogeneity and/or steep wetting fronts. Limitations can be minimized above all by installing a vertical single

TDR probe. This is the case with the earliest TDR waveguide developed by Topp and Davis (1985), which includes a series of changes in the diameter of the rods along their length, or the more complex probe designed by Hook et al. (1992), in which probe segmentation is achieved by using electronically switched shorting diodes. However, these single probes provide a limited number of depth intervals for determining the soil water content profile. More recently, Ferré et al. (1998) have designed a profiling probe that measures θ through two parallel access tubes. Although this probe allows for water content measurement over a specific depth interval equal to the rod length, it requires the manual placement of the rods for each depth increment. In addition, this probe design has the same limitations as apply to coated-rod TDR probes (Ferré and Topp, 2002).

As an alternative to the standard waveform analysis, Pereira dos Santos (1997) proposed a method for determining soil water content profiles by the inversion of a single TDR signal. However, although this method has shown a good performance, there are still limitations regarding the quality of the recovered signals (Sánchez-Pérez et al., 1999). The objective of this study was to investigate a new graphical interpretation of TDR reflected waveforms in non-conducting media that determines the variation in the apparent dielectric constant along a single TDR probe. The application of this waveform analysis procedure was specifically evaluated for profiling water content in soils.

2. MATERIALS AND METHODS

2.1. Theory

2.1.1. The relationships between the dielectric constant, impedance and the reflection coefficient

In TDR, a fast-rise step voltage electromagnetic pulse is propagated in the medium of interest along a transmission line. The cable tester records a TDR waveform type expressed by the voltage (V) or reflection coefficient (ρ) as function of time (t) (Fig. 1a). For an idealized medium, the

TDR waveform is a hypothetical trace that would occur if the media were non-conductive and perfectly homogeneous along the transmission line.

The transit time, t (s), of the TDR pulse propagating one return trip along a transmission line (e.g. a TDR probe) of length L (m) (Topp et al., 1980; Dalton et al., 1984) is represented by

$$t = \frac{2L\sqrt{K^*}}{c} \tag{1}$$

where c is the velocity of light in free space (3×10^8 m s^{-1}) and K^* the relative dielectric constant of the media.

The relative dielectric constant is treated as a complex form with a real part and an imaginary or dielectric loss component. The energy dissipation occurs through two processes. The first results from the polarization of dipolar molecules, which gives rise to a phase lag between the imposed field and the material's response to it. This phase lag is a function of the angular frequency, ω, of the imposed field. Because of this lag, the relative dielectric constant, K^*, must be represented as a complex quantity with real (in-phase), $K'(\omega)$, and imaginary (out-of-phase), $K''(\omega)$, components. The second process of energy dissipation arises from the electrical conductivity (EC), σ, of the media. The contribution of both polarization and conductivity to K^* is represented by (Kraus, 1984)

$$K^* = K'(\omega) - i\left(K''(\omega) + \frac{\sigma_0}{\omega K_0}\right) \tag{2}$$

where $i = \sqrt{-1}$, σ_0 is the zero frequency EC of the bulk sample, and K_0 is the dielectric constant of free space.

Over the TDR frequency range, most soils show a negligible dielectric loss, and hence $K^* \cong K'$. In these cases, the term "apparent dielectric constant" (K) can be used for the measured complex dielectric constant (Topp et al., 1980), and hence $K^* \cong K$.

When a transmission line with characteristic impedance Z_0 is immersed in a uniform material (soil or solution), its impedance Z_s is given by:

$$Z_s = \frac{Z_0}{\sqrt{K}} \qquad (2)$$

The characteristic impedance, Z_0, of an ideal coaxial transmission line depends only on the geometry of the line (Kraus, 1984):

$$Z_0 = 60 \ln(s/d) \qquad (3)$$

where s and d are the diameters of the outer and the inner conductors, respectively. Alternatively, Z_0 can be measured by determining the line's reflection coefficient ρ when the line is immersed in a uniform dielectric material of dielectric constant K (Kraus, 1984; Zegelin et al., 1989):

$$Z_0 = Z_r \sqrt{K} \left(\frac{1+\rho}{1-\rho} \right) \qquad (4)$$

where Z_r is the output impedance of the TDR cable tester. According to Zegelin et al. (1989), the more closely a non-coaxial transmission line (e.g. a TDR probe) emulates a coaxial line, the closer the Z_0 values obtained from Eqs. (3) and (4) would be.

In turn, ρ can be expressed as an impedance relationship (Topp et al., 1988). When an immersed transmission line is connected to a TDR system with an output impedance Z_r, the mismatched impedance of Z_r versus Z_s causes part of the input signal to be reflected back to the TDR, the remainder of the signal being transmitted into the sample (Topp et al., 1988). In this case, ρ can be defined as the ratio of the reflected signal amplitude to the incoming TDR signal amplitude (Kraus, 1984):

$$\rho = \frac{Z_s - Z_r}{Z_s + Z_r} \qquad -1 \le \rho \le +1 \qquad (5)$$

Alternatively, ρ can be written in the form

$$\rho = \left(\frac{V_1}{V_0} \right) - 1 \qquad (6)$$

where V_0 is the signal amplitude from the TDR device and V_1 the amplitude of the signal after partial reflection from the start of the probe (Zegelin et al., 1989).

Electromagnetic signals propagating in conductive media or solutions undergo attenuation. In an attenuating medium the magnitude of the signal decreases by the factor $exp(-\alpha x)$ as the signal propagates in a positive x direction (Kraus, 1984). The attenuation factor, f, is given as

$$f = \exp(-\alpha L) \tag{7}$$

where α is the attenuation constant

$$\alpha = 60\pi\left(\omega K_0 K'' + \sigma_{dc}\right) / K^{1/2} \tag{8}$$

and σ_{dc} is the static conductivity (Topp et al, 1980).

In conductive media, the reflection coefficient for the first round trip along the TDR probe of length L and back is given as (Yunuka et al., 1988)

$$\rho = \left(\frac{V_1}{V_0 f}\right) - 1 \tag{9}$$

This attenuation of ρ due to the medium EC can be avoided by insulating the TDR transmission lines with non-conductive materials (Mojid et al., 1998; Ferré et al., 2000, Fujiyasu et al., 2004).

2.1.2. *Dependence of the reflection coefficient and time of a TDR pulse on the dielectric constant*

Another procedure for measuring K by TDR in a non-conductive medium could be based on the dependence of both ρ and t on K. Combining Eqs. (1), (2) and (5) and solving for a section of apparent length l of an ideal coaxial TDR transmission line of total length L (L=nl), we obtain the following relationship:

$$\rho = \frac{Z_0 2l - Z_r c t_l}{Z_0 2l + Z_r c t_l} \tag{10}$$

describing the variation of ρ as a function of t for a given length l, t_l (Fig.1a). When this function, which starts at t_o = 0 (i.e. the first reflection or peak in a typical TDR waveform signature), is plotted together with a measured TDR waveform, the time for the intersection point of both curves (t_{1l}) is the time that the TDR pulse needs to travel an apparent length l along the whole TDR line (Fig. 1a). Similarly, the function defined by Eq. (10) for $t = t_{1l}$ intercepts the TDR waveform at time t_{2l}, which is the time taken for the pulse to travel a distance 2l. By repeating this procedure in an iterative way, we obtain a series of $\rho(t)$ lines intercepting the TDR trace at times t_{3l}, t_{4l},......and t_{nl} (Fig. 1b). These t values correspond to the time required for the TDR pulse to travel along the transmission line a distance 3l, 4l, ... and nl, respectively.

According to this approach and nomogram-like representation, hereafter called the *nomograph* (*NG*) method, we may rewrite Eq. (1)

$$K_i = \left(\frac{ct_{il}}{2(il)} \right)^2 \qquad \text{i=1,2,3,....n} \qquad (11)$$

to calculate the dielectric constant K_i of the medium for each il section of a TDR probe of total length L ($L=nl$). Also, K for the different l depth intervals, $K_{\Delta i}$, can be calculated as

$$K_{\Delta i} = \left(\frac{c\left(t_{il} - t_{(i-1)l}\right)}{2l} \right)^2 \qquad \text{i=1,2,3,....n} \qquad (12)$$

where $t_{(i-1)l}$ is the travel time for an apparent length $(i-1)l$.

2.2. TDR measurements

In the present study, TDR measurements were taken using a Tektronix model 1502C cable tester. A 1.5-m 50-Ω coaxial cable connected the TDR probes to the TDR pulser. TDR waveforms were transferred to a computer through a RS232 cable interface for display and analysis using the software WinTDR’98 (Or et al., 1998). K and Z_0 were automatically calculated using the double reflection procedure and Eq. (4), respectively.

Similarly, ρ was calculated from Eq. (6), where V_0 and V_1 were obtained from the TDR trace output as

$$V_0 = Px_{50\Omega} - Px_{0\Omega} \quad (13)$$

$$V_1 = Px_t - Px_{0\Omega} \quad (14)$$

where $Px_{50\Omega}$ and $Px_{0\Omega}$ are the TDR waveform output in pixels for the 50 and 0 Ω values, respectively, and Px_t the pixel value for Ω at a given t on the TDR waveform (Or et al., 1998).

2.3. Experimental design

A first experiment was performed to evaluate the influence of K on Z_0 in non-conductive media. To this end, six different types of TDR probes were tested: five three-wire probes with stainless steel rods of variable length and dimensions (probe P1, P2, P3, P4 and P5) and one coaxial-type probe (P6) (Table 1). The six TDR probes were individually immersed in eleven non-conducting homogeneous fluids (Table 2), contained in a cylindrical PVC container 60-cm high and 25-cm in internal diameter. The TDR sensors were separated far enough from the wall of the container to avoid air distortions during the measurements. The apparent dielectric constant, K, and the characteristic impedance, Z_0, were automatically calculated as described above.

A second experiment was carried out to validate the values of K measured using the *NG* method from Eq. (11) by comparing them with those obtained by the standard double-reflection procedure. To this end, two different probe geometries were studied in two different sand columns. For the first sand column, four uncoated TDR probes of type P1 (Table 1) of 10-, 20-, 30-, and 40-cm length were vertically placed into a cylindrical clear plastic container (25-cm in internal diameter and 60-cm in height) before filling it with sand. The probe heads rested at the top surface of the container, and all of them were separated at least 5 cm from one another and from the wall of the container to avoid distortions during the measurements. A 1.2-m long coaxial cable connected the TDR probes to a multiplexer (Campbell Scientific Inc., model SDMX50), which transferred the signal to the cable tester. The container, which had a drain valve at the bottom, was filled up to 1 cm above the base of the vertical TDR probes' heads with air-dry coarse commercial sand (630 μm average grain size). The sand column was poured in by hand and gently tapped in small incremental steps to achieve a uniform bulk density. The initial sand column volumetric water content was 0.061 $m^3 m^{-3}$. The column was then saturated with distilled water through capillary wetting from the bottom. The capillary wetting procedure was apparently uniform throughout the experiment. Afterwards, the column was slowly drained out using a vacuum hand pump operating at a maximum suction of 60 kPa. TDR measurements of K were taken at regular intervals of time throughout the wetting and draining cycle.

For the second sand column, tests were performed with eight TDR probes of type P5 of variable length, which were placed into a cylindrical clear PVC container (40-cm in internal diameter and 75-cm in height) before filling it with sand. Four 10-cm long probes were positioned horizontally at 10, 20, 40 and 50 cm depth. The other four TDR probes, which were 10-, 20-, 40-, and 60-cm long, were placed vertically with the probe heads resting at the top surface of the container. All the probes were separated at least 8 cm from one another and from the wall of the container. The probe rods were insulated with polyolefin heat-shrink tubing with a wall thickness of 0.2 mm. A 1.5-m long coaxial cable connected the TDR probes to a multiplexer. The PVC container, which had a drain valve at the bottom, was filled with air-dry coarse commercial sand (630 μm average grain size). The sand column was packed in small incremental steps to achieve a uniform bulk density (an average value of 1.42 g cm^{-3}). The initial sand column volumetric water content was 0.084 $m^3 m^{-3}$ The column was then saturated with distilled water through capillary wetting from the bottom. Afterwards, the column was slowly drained. TDR measurements of K were taken with both vertical and horizontal probes at regular intervals of time throughout the wetting and draining cycle. The intercept points between the $\rho(t)$ lines and the current TDR waveforms (Fig. 1b) for the NG method were automatically determined as the minimum distance between both curves.

To evaluate the effect of the rod coating of polyolefin heat-shrink tubing on K and consequently on the volumetric soil water content (θ), two 10-cm long three-rod probes, one with coated rods and the other with uncoated rods, were simultaneously immersed into a PVC column 20-cm high and 20-cm in internal diameter filled up with sand. TDR measurements were then taken for 10 different soil water contents. The calibration relationship between the values of K obtained with the uncoated probe (K_{uncoat}) and the values obtained with the coated probe (K_{coat}) resulted in

$$K_{uncoat} = 0.0108\ (K_{coat})^2 + 1.4942\ K_{coat} - 0.8297 \qquad (15)$$

with a coefficient of determination (R^2) of 0.98. The volumetric water content was then calculated using the K_{uncoat} values and the equation proposed by Topp et al. (1980).

3. RESULTS AND DISCUSSION

3.1. Dependence of Z_0 on K in non-conducting media

Figure 2a shows the relationship between Z_0 and K for the media and six TDR probe geometries tested (Table 1). Compared to the Z_0 measured for the three-rod TDR probes (P1, P2, P3, P4 and P5), Z_0 for the coaxial TDR sensor (probe P6) did not vary significantly with K, showing values close to the Z_0 value (102.3) obtained from Eq. (3) for this probe. These results are in line with those obtained by Zegelin et al. (1989), who compared the characteristic impedance of coaxial and three- and four-wire probes. In our study, the differences in Z_0 for each K value among the five types of three-wire probes may be due to the effect of probe geometry on Z_0. This is illustrated by Fig. 2b, which shows how these differences tend to disappear when Z_0 is divided by the geometry factor, $ln(s/d)$, and plotted against K.

When examining the above results just for the range between the minimum and maximum K values measured in the two sand columns, it was found that the best relationship between the K and Z_0 for three-wire TDR probes, $Z_{0(P)}$, differed according to the probe geometry. The best $Z_{0(P)}$

for the TDR probe of type P1 and K values between 3 and 30, $Z_{0(P1)}$, was expressed according to the following best fit equation

$$Z_{0(P1)} = \left(64.75 + 0.82K - 0.0056K^2\right)\ln\left(\frac{s}{d}\right) \qquad (R^2 = 0.972) \qquad (16)$$

In contrast, for the probe P5 and the range of K values from 3 to 20, the best $Z_{0(P5)}$ fit function was

$$Z_{0(P5)} = \left(66 + 1.2\ln(K)\right)\ln\left(\frac{s}{d}\right) \qquad (R^2 = 0.985) \qquad (17)$$

These differences indicate that probe geometry has an influence on the relationship between Z_0 and K.

3.2. Validation of the *NG* waveform analysis approach

The theoretical relationship between ρ and t for an ideal coaxial line given by Eq. (10) was adapted to three-rod TDR probes of type P1 and P5 by substituting Z_0 in Eq. (10) with $Z_{0(P)}$ obtained from Eq. (16) and Eq. (17), respectively. Taking into account that the lowest practical TDR probe length for water content measurement is about 10 cm (Dalton and van Genuchten, 1986), the $\rho(t)$ line for both a 10-cm long ideal coaxial probe and a 10-cm long three-wire TDR probe were calculated. These lines were plotted together with the experimental TDR waveforms obtained with a 10-cm long three-wire probe in the sand column from air-dry to saturation ($K \approx$ 3-30) (Fig. 3). Compared to the ideal coaxial $\rho(t)$ line, the $\rho(t)$ line for the three-rod probe of type P5 intersects the experimental waveforms at exactly the second reflection point (i.e. the minimum value of ρ). This finding indicates that when the theoretical *NG* method is applied to a three-rod probe, a specific correction for Z_0 has to be made in order to obtain reliable K readings.

Figure 4a shows an example of TDR waveforms obtained from measurements taken with vertical 10-, 20-, 40-, and 60-cm long three-wire probes of type P5 for a given water content distribution in the sand column. The waveforms for short TDR probes overlap those of longer probes, which indicates that the TDR trace of the longest probe contains the information supplied by signatures from shorter probes. Hence, the K profile of a given medium can in principle be determined using a single long TDR probe. The corrected $\rho(t)$ function for a three-rod probe of l=10 cm (Eq. 10) was iteratively calculated for 10, 20, 30, 40, 50 and 60 cm length and plotted along with waveforms for 10-, 20-, 40-, and 60-cm long TDR probes (Fig. 4b). As can be seen, the $\rho(t)$ lines for 10, 20, 40 and 60 cm intercept the experimental TDR waveforms for the same probe length at the second reflection point. This fact indicates that the *NG* method is fairly consistent for measuring K profiles using Eq. (12), because it accurately measures the t_{il} values for 10-cm intervals along the 60-cm long TDR probe.

In order to further test the robustness of the *NG* method, a total of 32 values of K (8 samplings) measured in the sand column during the first wetting and drainage cycle with the vertical 10-, 20-, 30-, and 40-cm long TDR probes of type P1 according to the double reflection waveform analysis were correlated with the K values for the same depths obtained by the *NG* method (Eq. 11) applied to the 40-cm long TDR probe (Fig. 5). The same experiment was applied to the TDR probe of type P5 where a total of 112 values of K (28 samplings) were measured (Fig. 5). Overall, a very satisfactory correlation was observed between the two procedures (Fig. 5a, b), particularly for the 0-60-cm depth samplings (Fig. 5f). The standard deviation of the regression (SD) and the root mean standard error (RMSE) measured for the different TDR probes were low (Fig. 5). This result indicates that the *NG* method can satisfactorily be used for profiling the soil dielectric constant. The weaker correlation found for the 0-10, 0-20, and 0-40 cm depths (Fig. 5c, d, e) could be due to the spatial fluctuation of the wetting front within the sand column during the wetting and draining processes. By the same token, small air-gaps between the coating material (i.e. the polyolefin heat-shrink tubing) and the stainless steel rods could have altered the sensitivity of the probes. In this regard, Ferré et al. (1996) found that under variable water content conditions PVC-coated rods underestimate the average water contents while the presence of air-filled gaps constitutes another potential source of measurement error. The limitations associated with plastic tubing insulation materials could be alleviated by using acrylic spray paints (Fujiyasu et al., 2004).

The results from the specific experiment conducted to evaluate the suitability of the *NG* method for measuring the soil moisture profile using a single TDR probe are also quite promising. Figure 6 thus shows that soil water content measurements taken on the sand column at 10-cm intervals using the *NG* method applied to a 60-cm long TDR probe compare satisfactorily with those obtained by horizontal TDR probes inserted at 10, 20, 40 and 50 cm depth, even though the soil volume sampled by the two procedures is not exactly the same. The *NG* soil moisture profiles were calculated by applying the Topp et al. (1980) equation to the K_{uncoat} values, which in turn were derived from their relationship with the K_{coat} values (Eq. 15). The K obtained with the coated probe, K_{coat}, was determined at 10-cm intervals by Eq. (12) for l = 10 cm and t intervals delimited by the t_{il} waveform intersection points for two consecutive $\rho(t)$ lines (i.e. Fig. 1b). From a practical viewpoint, this procedure for estimating θ could be simplified by eliminating the step of determining the K_{coat} vs K_{uncoat} relationship through the use of TDR probes coated with high dielectric insulation materials, as recently proposed by Fujiyasu et al. (2004).

In conclusion, the TDR waveform analysis procedure here proposed has proven to be a robust and suitable method for determining the variation of K at fixed intervals along a single probe and accordingly for soil water content profiling. However, further research is needed to (i) quantify the error of the *NG* method in measuring K in heterogeneous media and (ii) find a general equation to describe the Z_0 vs K relationship for different geometries of three-wire TDR probes. These improvements would make it possible to standardize the use of the *NG* method for any three-wire TDR probe. Also, certain technical limitations for field application can be found with this method. Errors in the measurement of K can arise due to air-gaps between the coating material and the probe rods and/or surface abrasion of the rod coating material during the insertion of TDR probes in hard or gravelly soils. These could be avoided by using alternative coating materials (e.g. epoxy-ceramic nanocomposite) with different properties (e.g. thickness, abrasion resistance, durability) that would improve the sensitivity of the proposed method for field measurements of the soil water content profile using a single long TDR probe.

ACKNOWLEDGMENTS

This work was supported by the Comisión Interministerial de Ciencia y Tecnología of Spain (grants AGF98-0261-CO2-02 and AGL2001-2238-CO2-01). We gratefully acknowledge the support and thoughtful inputs of Prof. Dani Or (Environmental Physics Group, University of Connecticut) at the initial stage of this research.

REFERENCES

Dalton, F.N, van Genuchten, M.T., 1986. The time-domain reflectometry method for measuring soil water content and salinity. Geoderma 237-250.

Dalton, F.N., Herkelrath, W.N., Rawlins, D.S., Rhoades, J.D., 1984. Time-domain reflectometry: simultaneous measurement of soil water content and electrical conductivity with a single probe. Science 224, 989-990.

Ferré, P.A., Topp, G.C., 2002. Time Domain Reflectometry. In: Dane, J.H., Topp, G.C. (Eds). Methods of Soil Analysis. Part 4-Physical Methods, SSSA Book Series No. 5, Madison, WI, USA, pp. 434-446.

Ferré, P.A., Rudolph, D.L., Kachanoski, R.G., 1996. Spatial averaging of water content by time domain reflectometry: Implications for twin rod probes with and without dielectric coatings. Water Resour. Res. 32, 271-279.

Ferré, P.A., Rudolph, D.L., Kachanoski, R.G., 1998. Water content response of a profiling time domain reflectometry probe. Soil Sci. Soc. Am. J. 62, 865-873.

Ferré, P.A., Knight, J.H., Rudolph, D.L., Kachanoski, R.G., 2000. A numerically based analysis of the sensitivity of conventional and alternative time domain reflectometry probes. Water Resour. Res. 36, 2461-2468.

Fujiyasu, Y., Pierce, C.E., Fan, L., Wong, C.P., 2004. High dielectric insulation coating for time domain reflectometry soil moisture sensor. Water Resour. Res. 40, Art. No.W04602 APR 17 2004.

Herkelrath, W. N., Hamburg, S. P., Murphy, F., 1991. Automatic, real-time monitoring of soil moisture in a remote field area with time domain reflectometry. Water Resour. Res., 27, 857-864.

Hook, W.R., Livingston, N.J., Sun, Z.J., Hook, P.B., 1992. Remote diode shorting improves measurement of soil water by time domain reflectometry. Soil Sci. Soc. Am. J. 56, 1384-1391.

Kraus, J.D., 1984. Electromagnetics. 3rd ed., McGraw-Hill, New York.

Mojid, M.A., Wyseure, G.C.L., Rose, D.A., 1998. The use of insulated time-domain reflectometry sensors to measure water content in highly saline soils. Irrig. Sci., 18, 55-61.

Pereira dos Santos, L., 1997. Développment d'une nouvelle méthode de détermination des profils de tenuer en eau dans les sols par inversion d'un signal TDR. Thése de doctorat, Université Joseph Fourier, Grenoble, France.

Or, D., Fisher, B., Hubscher, R.A., Wraith, J., 1998. WinTDR 98 V.4.0 –Users Guide-. Department of Plants, Soil and Biometeorology, Utah State University, Logan, UT, USA.

Roth, K., Schulin, R., Fluhler, H., Attinger, W., 1990. Calibration of time domain reflectometry for water content measurement using a composite dielectric approach. Water Resour. Res., 26, 2267-2273.

Sánchez-Pérez, J.M., Laurent, J.P., Bohy, M., Auzet, A.V., Thony, J.L., 1999. Evaluación de un nuevo método de caracterización del perfil hídrico del suelo a partir de la inversión de una sola señal TDR. In: Muñoz-Carpena, R., Ritter, A., Tascón, C. (Eds.), Estudios en la Zona no Saturada del Suelo, ICIA, La Laguna, Spain, pp. 33-38.

Topp, G.C., Davis, J.L., 1985. Measurement of soil water content using time-domain reflectrometry (TDR): a field evaluation. Soil Sci. Soc. Am. J. 49, 19-24.

Topp, G.C., Davis, J.L., Annan, A.P., 1980. Electromagnetic determination of soil water content: measurements in coaxial transmission lines. Water Resour. Res. 16, 574-582.

Topp, G.C., Yanuka, M., Zebchuk, W.D., Zegelin, S., 1988. Determination of electrical conductivity using time domain reflectometry: soil and water experiments in coaxial lines. Water Resour. Res. 24, 945-952.

Yu, C., Warrick, A.W., Conklin, M.H., Young, M.H., Zreda, M., 1997. Two- and three-parameter calibrations of time domain reflectometry for soil moisture measurement. Water Resour. Res. 33, 2417-2421.

Yanuka, M., Topp, G.C., Zegelin, S., Zebchuk, W.D. 1988. Multiple reflection and attenuation of time domain reflectometry pulses: theoretical considerations for applications to soil and water. Water Resour. Res. 24, 939-944.

Zegelin, S.J., White, I., Jenkins, D.R., 1989. Improved field probes for soil water content and electrical conductivity measurement using time domain reflectometry. Water Resour. Res. 25, 2367-2376.

FIGURE CAPTIONS

Fig. 1. Graphical representation of an idealized TDR waveform from a probe of length L ($L=nl$) along with (a) the $\rho(t)$ line (*NG* method) for an initial length $1l$ intercepting the TDR trace at time t_{1l} and (b) subsequent $\rho(t)$ lines crossing the waveform at times t_{2l}, t_{3l},......and t_{nl}.

Fig. 2. Relationship between the dielectric constant K of different non-conducting media (Table 2) and the characteristic impedance Z_0 (a) and the ratio $Z_0/ln(s/d)$ (b) for TDR probes with different geometry (Table 1) (*s*: spacing of the outer probe conductors; *d*: diameter of the inner conductors).

Fig. 3. $\rho(t)$ line for a 10-cm long ideal coaxial probe and adjusted line for a 10-cm long three-wire TDR probe of type P5 (Table 1) intercepting experimental TDR waveforms from measurements taken in the sand column with a 10-cm long three-wire probe from air-dry to saturation ($K \approx$3-30).

Fig. 4. (a) Example of TDR waveforms from 10-, 20-, 40-, and 60-cm long three-wire probes of type P5 (Table 1) vertically inserted in the sand column and (b) their interceptions with the three-wire probe $\rho(t)$ lines for 10, 20, 30, 40, 50 and 60 cm depth.

Fig. 5. Relationship between the dielectric constant (K) measured in the sand column by TDR (tangent method) using TDR probes of type P1 of 10-, 20-, 30-, and 40-cm lengths and TDR probes of type P5 of 10-, 20-, 40- and 60-cm lengths (Table 1) and that given by the nomograph method as applied to the 40- and 60-cm long TDR probe, respectively.

Fig. 6. Comparison of volumetric water content (θ) in the sand column profile measured throughout the wetting and drainage cycle using horizontal TDR probes placed at 10, 20, 40,

and 50 cm depth (●) with the θ profile obtained from the nomograph method for the TDR probe of type P5 (Table 1) at 0-10, 10-20, 30-40, 40-50 and 50-60 cm depth intervals (○).

Table 1. Geometry of the TDR probes used to test the influence of the dielectric constant of the medium on the characteristic probe impedance.

Probe dimensions	Three-rod probes					Coaxial probe
	P1	P2	P3	P4	P5	P6
Spacing of the outer conductor (*s*) (mm)	28.0	36.5	17.3	16.3	83	35.0
Rod diameter (*d*) (mm)	3.2	5.0	2.4	3.2	10	6.4
s/d	8.7	7.3	7.2	5.1	8.3	5.5
Probe length (*L*) (mm)	200	200	100	185	200	195

Table 2. Nonconducting fluids used to test the influence of the dielectric constant of the medium on the characteristic probe impedance.

Fluid	Dielectric constant
Air	1.05
Sunflower oil	2.42
Acetic acid	9.22
Aqueous acetic acid solution (60:40, *v/v*)	15.76
Ethanol	21.39
Aqueous ethanol solution (90:10, *v/v*)	26.62
Aqueous ethanol solution (85:15, *v/v*)	31.53
Aqueous ethanol solution (70:30, *v/v*)	40.65
Aqueous ethanol solution (50:50, *v/v*)	51.41
Aqueous ethanol solution (35:65, *v/v*)	61.23
Distilled water	80.22

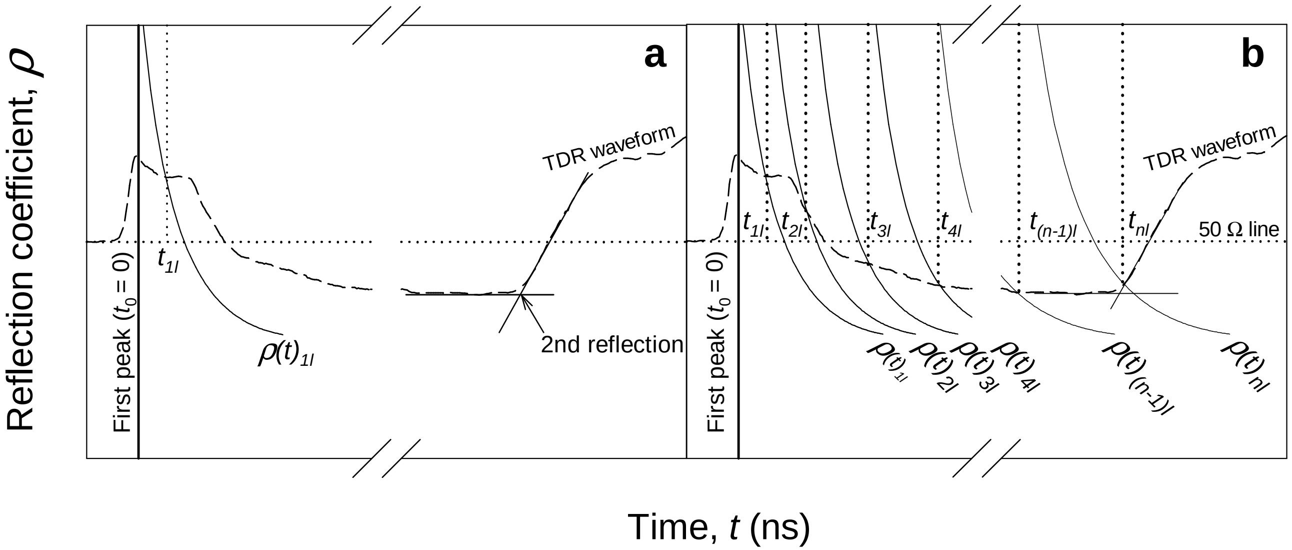

Reflection coefficient, ρ
a
b
TDR waveform
First peak (t_0 = 0)
t_{1l}
$\rho(t)_{1l}$
2nd reflection
t_{2l}
t_{3l}
t_{4l}
$t_{(n-1)l}$
t_{nl}
50 Ω line
$\rho(t)_{2l}$
$\rho(t)_{3l}$
$\rho(t)_{4l}$
$\rho(t)_{(n-1)l}$
$\rho(t)_{nl}$
Time, t (ns)

Fig.1

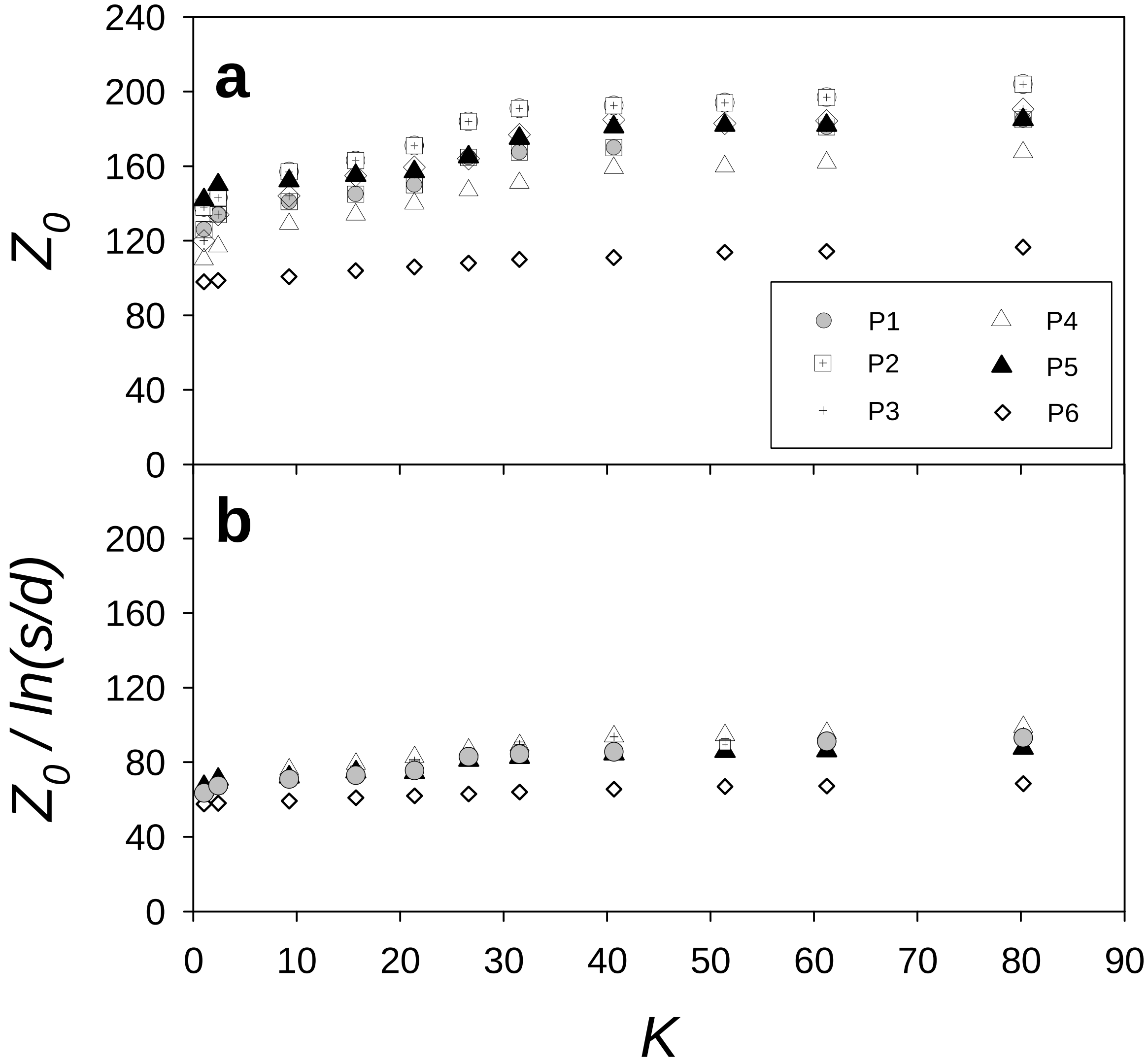
a
b
240
200
160
120
80
40
0
Z_0
Z_0 / ln(s/d)
P1
P2
P3
P4
P5
P6
0
10
20
30
40
50
60
70
80
90
K

Fig.2

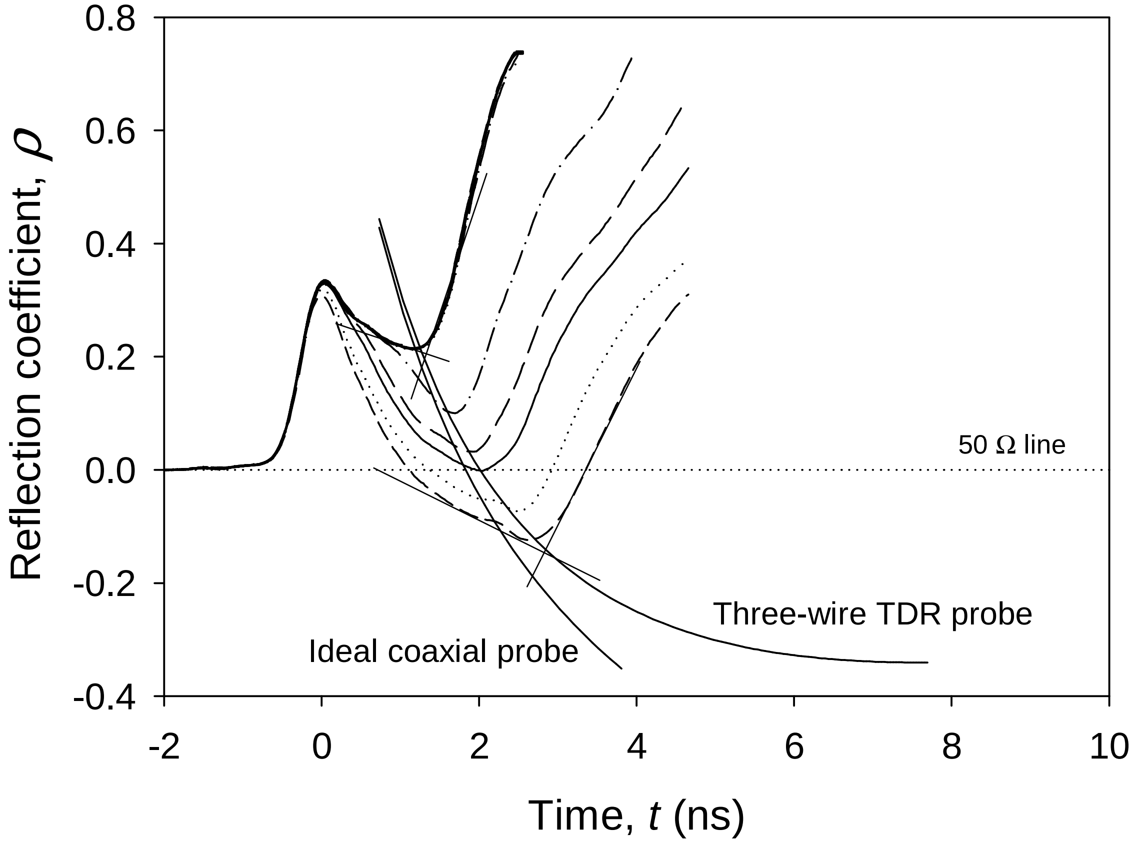
Reflection coefficient, ρ
Time, t (ns)
50 Ω line
Three-wire TDR probe
Ideal coaxial probe
0.8
0.6
0.4
0.2
0.0
-0.2
-0.4
-2
0
2
4
6
8
10

Fig.3

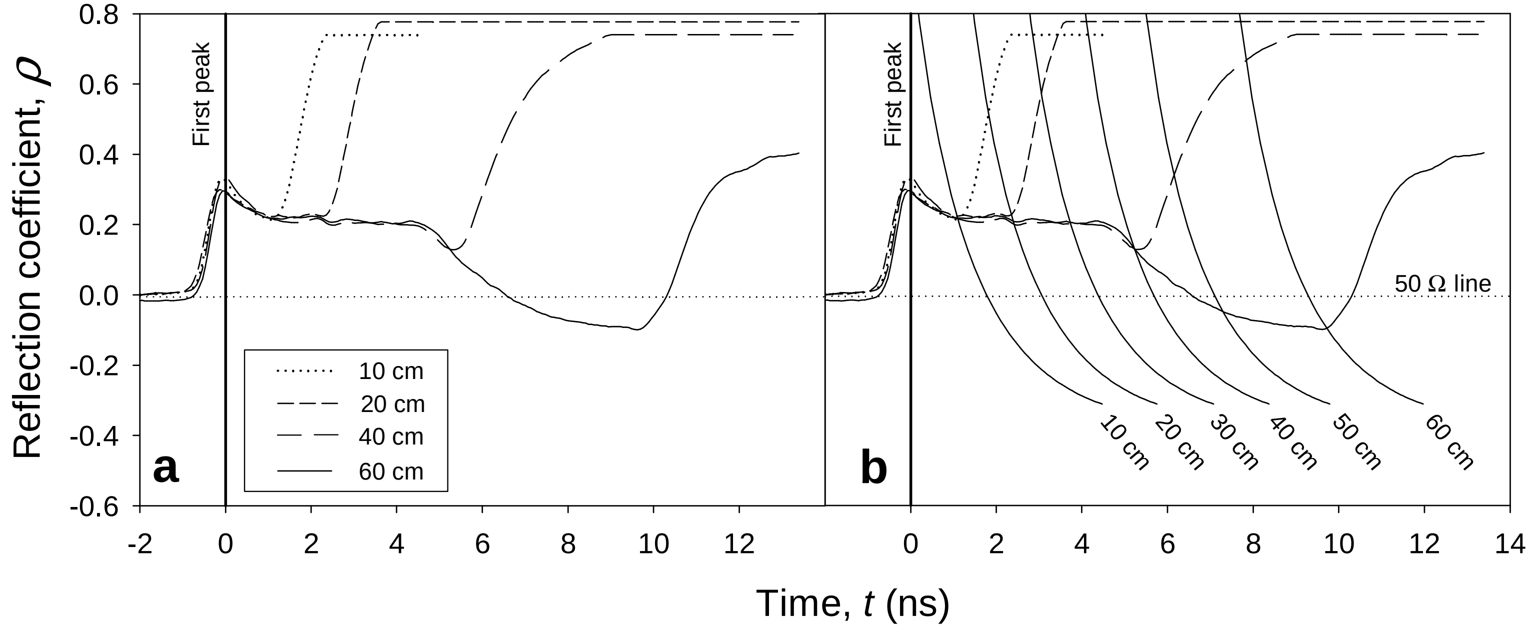

Reflection coefficient, ρ
Time, t (ns)
First peak
First peak
a
b
10 cm
20 cm
40 cm
60 cm
50 Ω line
10 cm
20 cm
30 cm
40 cm
50 cm
60 cm

Fig.4

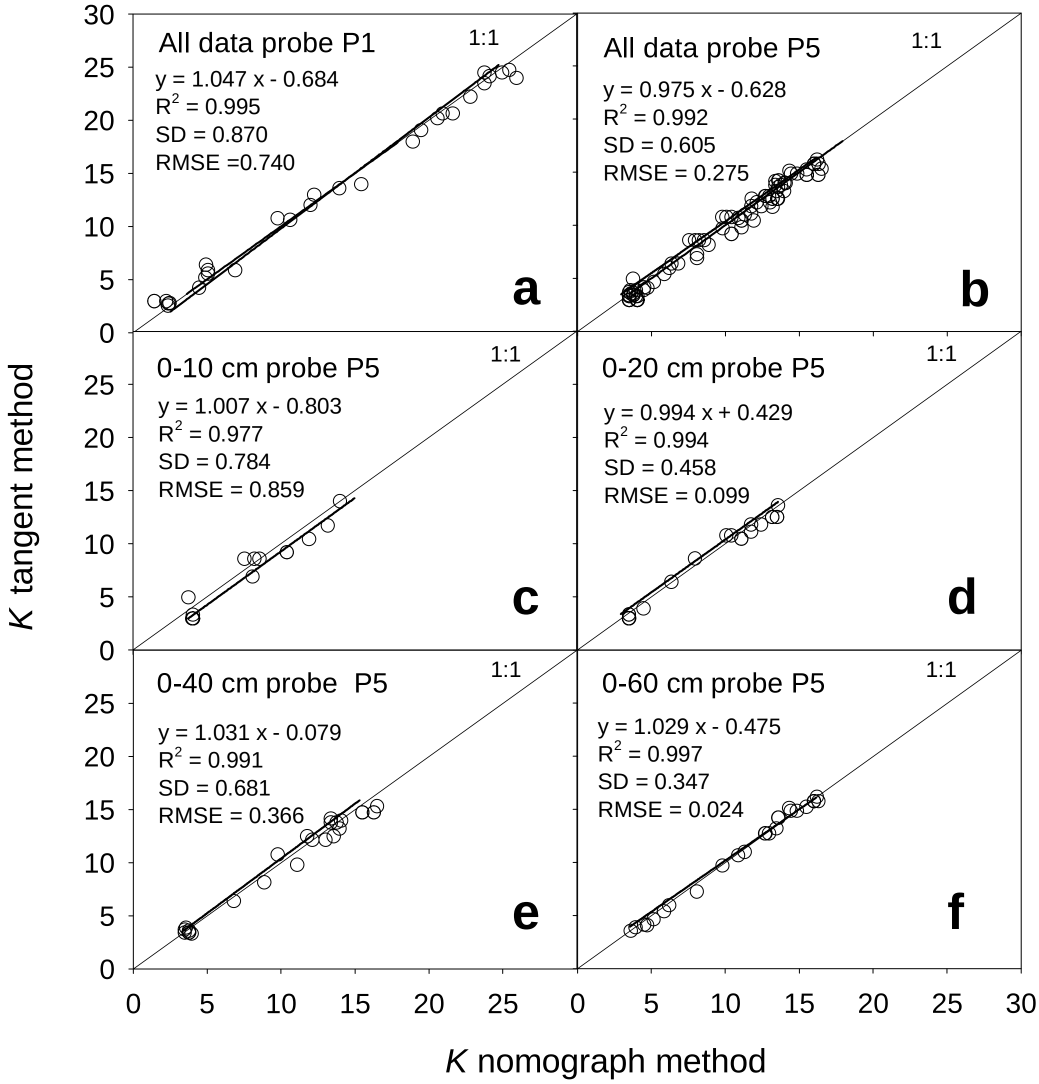
All data probe P1
1:1
y = 1.047 x - 0.684
R2 = 0.995
SD = 0.870
RMSE =0.740
a
All data probe P5
1:1
y = 0.975 x - 0.628
R2 = 0.992
SD = 0.605
RMSE = 0.275
b
0-10 cm probe P5
1:1
y = 1.007 x - 0.803
R2 = 0.977
SD = 0.784
RMSE = 0.859
c
0-20 cm probe P5
1:1
y = 0.994 x + 0.429
R2 = 0.994
SD = 0.458
RMSE = 0.099
d
0-40 cm probe P5
1:1
y = 1.031 x - 0.079
R2 = 0.991
SD = 0.681
RMSE = 0.366
e
0-60 cm probe P5
1:1
y = 1.029 x - 0.475
R2 = 0.997
SD = 0.347
RMSE = 0.024
f
K tangent method
K nomograph method

Fig.5

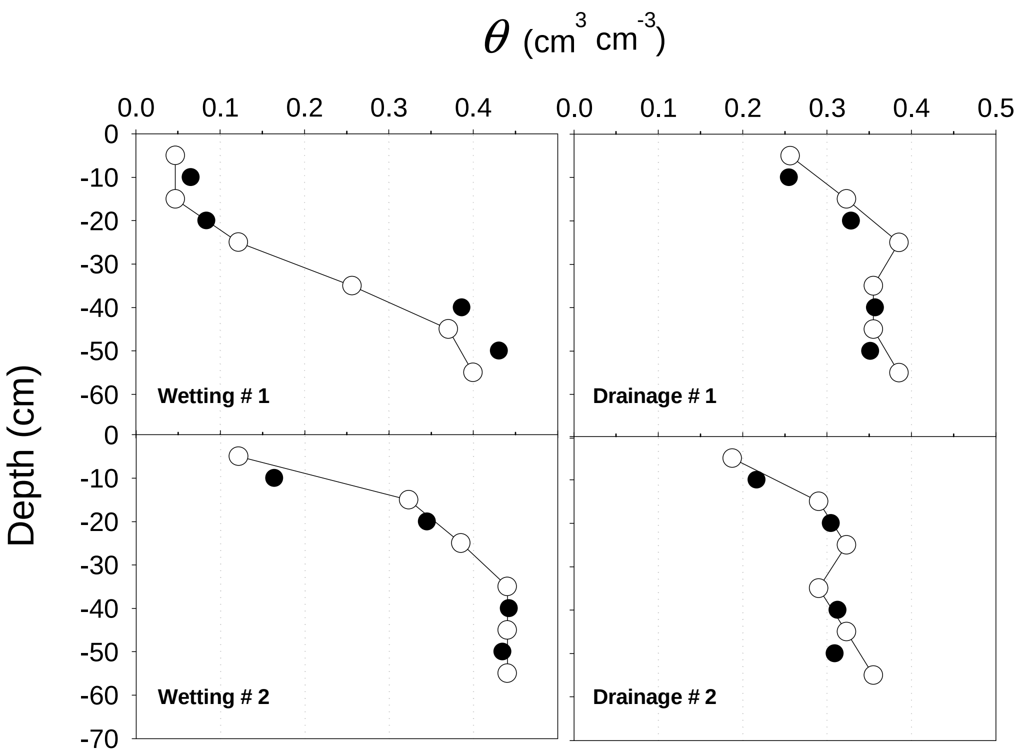

θ (cm^3 cm^{-3})
Depth (cm)
0.0
0.1
0.2
0.3
0.4
0.5
0
-10
-20
-30
-40
-50
-60
-70
Wetting # 1
Drainage # 1
Wetting # 2
Drainage # 2

Fig.6